

UNCERTAINTY-AWARE 3D EMOTIONAL TALKING FACE SYNTHESIS WITH EMOTION PRIOR DISTILLATION

Nanhan Shen and Zhilei Liu*

School of Artificial Intelligence, Tianjin University, Tianjin, China

ABSTRACT

Emotional Talking Face synthesis is pivotal in multimedia and signal processing, yet existing 3D methods suffer from two critical challenges: poor audio-vision emotion alignment, manifested as difficult audio emotion extraction and inadequate control over emotional micro-expressions; and a one-size-fits-all multi-view fusion strategy that overlooks uncertainty and feature quality differences, undermining rendering quality. We propose UA-3DTalk, Uncertainty-Aware 3D Emotional Talking Face Synthesis with emotion prior distillation, which has three core modules: the Prior Extraction module disentangles audio into content-synchronized features for alignment and person-specific complementary features for individualization; the Emotion Distillation module introduces a multi-modal attention-weighted fusion mechanism and 4D Gaussian encoding with multi-resolution code-books, enabling fine-grained audio emotion extraction and precise control of emotional micro-expressions; the Uncertainty-based Deformation deploys uncertainty blocks to estimate view-specific aleatoric (input noise) and epistemic (model parameters) uncertainty, realizing adaptive multi-view fusion and incorporating a multi-head decoder for Gaussian primitive optimization to mitigate the limitations of uniform-weight fusion. Extensive experiments on regular and emotional datasets show UA-3DTalk outperforms state-of-the-art methods like DEGSTalk and EDTalk by 5.2% in E-FID for emotion alignment, 3.1% in SyncC for lip synchronization, and 0.015 in LPIPS for rendering quality. Project page: <https://mrask999.github.io/UA-3DTalk/>.

Index Terms— Talking Face Synthesis, Uncertainty Estimation, 3D Gaussian Splatting, Emotion Synthesis, Lip Synchronization

1. INTRODUCTION

Emotional talking face synthesis has become a hot research field in multimedia and signal processing, due to its wide range of utilities[1]. Current methods mainly suffer from two aspects of technical challenges, each with non-trivial limitations. The introduction of emotion leads to the first challenge. Firstly, unlike traditional talking face, exaggerated mouth movements or expressions are common in this scenario, which demands higher synchronization accuracy [2]. Secondly, audio emotion extraction itself is a challenge, as this is also a hot topic in Speech Emotion Recognition(SER). Current works mainly rely on reference-based emotion control (e.g., EmotiveTalk[3]), which is dependent on high-quality reference video clips and unsatisfactory in pure audio-driven scenarios. Last but not least, compared to the traditional talking face, this demands stronger control over expressions from audio, which cannot be fully satisfied by the former methods. The second challenge lies in the multi-view feature fusion, which is always overlooked. Usually, a

flawed "one-size-fits-all" strategy is implemented that concatenates all features together [4][5][6], which may generate feature inputs with a length of several hundred dimensions. In practice, modality quality varies drastically due to occlusions, representation learning issues, and noise; ignoring these differences and inherent uncertainty in multi-view data yields suboptimal results. To address these challenges, we propose UA-3DTalk (Uncertainty-Aware 3D Emotional Talking Face Synthesis with Emotion Prior Distillation), a framework that adopts 3D Gaussian Splatting (3DGS) as its rendering backbone and comprises three core modules: Prior Extraction, Emotion Distillation, and Uncertainty-based Deformation.

The implementation of Prior Extraction and Emotion Distillation is fundamental in addressing the issue of poor audio-vision emotion alignment. In Prior Extraction, we disentangled the audio into f_{exp} and f_{tone} as [7]. f_{exp} is a content-synchronized feature for audio-vis alignment and f_{tone} is a person-specific complementary feature for individualization, Jointly ensuring synchronization and identity precision. In Emotion Distillation, we extend the audio window and adopt multi-modal fusion to capture sufficient emotion information without feature dilution. We extract spectrogram, MFCC, and audio-wav from audio, use the first two as attention keys to re-weight the third for emotion classification and expression prediction [8], then encode the emotion features via multi-plane gridding [9] and multi-resolution code-books [10] for precise control of emotional expressions.

The Uncertainty-based Deformation module has been proposed as a solution to the problem of suboptimal one-size-fits-all multi-view fusion in existing 3D emotional talking face synthesis methods, uncertainty blocks are implemented for each feature view to jointly generate a state vector for each Gaussian primitive. Unlike previous works such as [11], these blocks separately estimate aleatoric uncertainty (AU) from input noise and epistemic uncertainty (EU) from model parameters and predict view-specific state vectors [12, 13]. Adaptive fusion is then implemented based on this information with the rule: higher uncertainty leads to lower view weight. The generated state vector is decoded by a multi-head Gaussian deformation decoder [9] to output modifications of Gaussian primitives. Furthermore, it facilitates the initial systematic integration of uncertainty modeling in the domain of talking face generation.

In conclusion, main contributions of our work can be summarized as:

- To address the flawed multi-view fusion issue, we are the first to systematically model aleatoric and epistemic uncertainty in 3D emotional talking face synthesis.
- We propose an uncertainty-aware adaptive fusion strategy, which dynamically adjusts view weights based on feature quality, prioritizing low-uncertainty information.
- The Emotion Prior Distillation leverages both the Prior Extraction module and the Emotion Distillation module in a collaborative manner to address the emotion alignment problem.

*Corresponding author (zhileiliu@tju.edu.cn)

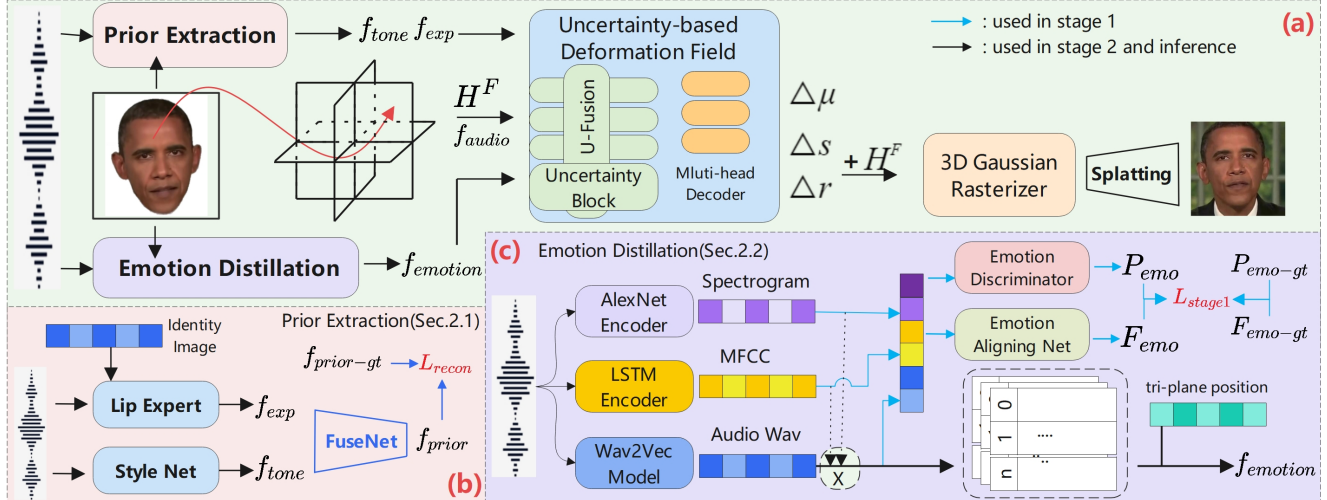


Fig. 1: Overall architecture of the proposed UA-3DTalk framework: (a) End-to-end pipeline of the face branch, integrating Prior Extraction, Emotion Distillation, and Uncertainty-based Deformation for 3D Gaussian primitive adjustment and rendering; (b) Detailed framework of the Prior Extraction module; (c) Technical pipeline of the Emotion Distillation module.

2. PROPOSED METHOD

The architecture of our UA-3DTalk is shown in Fig. 1, in which 3DGS is adopted as the rendering backbone. Input image and audio are fed into the Prior Extraction module (Fig. 1(b)) to generate f_{exp} , f_{tone} and into the Emotion Distillation module (Fig. 1(c)) to obtain $f_{emotion}$. These features, together with static Gaussian primitives H and the baseline’s simply encoded audio feature f_{audio} [5], are input to the Uncertainty-based Deformation module to compute modifications for Gaussian primitives. The Gaussian rasterizer then uses these modified primitives to render dynamic facial frames. Consistent with [5], we decompose the head into face and mouth branches; the above pipeline corresponds to the face branch (Fig. 1(a)).

In 3DGS, static gaussian primitives, which model the human head, are defined by a set of point cloud parameters: a 3D center $\mu \in \mathbb{R}^3$, a 3D scaling factor $s \in \mathbb{R}^3$, a 4D rotation quaternion $r \in \mathbb{R}^4$, a scalar opacity value $\alpha \in \mathbb{R}$, and a Z -dimensional color feature $c \in \mathbb{R}^Z$. The covariance matrix Σ is derived from s and r . For pixel-level color rendering, the target pixel’s color C is computed by blending contributions from N ordered Gaussian primitives that overlap with the pixel, following Eqs. 1 and 2.

$$C = \sum_{i \in \mathcal{N}} c_i \alpha_i \prod_{j=1}^{i-1} (1 - \alpha_j), \quad \alpha_i = \sigma_i \mathcal{G}_i(\mathbf{x}) \quad (1)$$

$$\mathcal{G}_i(\mathbf{x}) = e^{-\frac{1}{2}(\mathbf{x} - \boldsymbol{\mu}_i)^T \Sigma_i^{-1} (\mathbf{x} - \boldsymbol{\mu}_i)} \quad (2)$$

where $\mathcal{G}_i(\mathbf{x})$ denotes the Gaussian distribution value of the i -th primitive at the pixel position \mathbf{x} , and σ_i is a scaling coefficient for the i -th primitive’s opacity. To render dynamic facial images, we introduce a deformation field $\delta_i = \{\Delta\mu_i, \Delta s_i, \Delta r_i\}$, representing modifications to the Gaussian primitives’ position, scaling, and rotation, respectively. This deformation field is defined in Eq. 3:

$$\delta_i = \text{Deformation}(\mathcal{H}, f_{audio}, f_{exp}, f_{tone}, f_{emotion}) \quad (3)$$

It is notable that the pipeline of the mouth branch differs slightly from that of the face branch: it excludes the emotional feature $f_{emotion}$ from the input of the deformation field, and the deformation field only outputs the position modification $\Delta\mu$ for Gaussian primitives. All other components remain consistent with those of the face branch.

2.1. Prior Extraction

To satisfy the elevated requirements of audio-vision synchronization and identity preservation in emotional talking face, the Prior Extraction module is utilized for the generation of highly audio-vision synchronized expression features f_{exp} and person-specific complementary information f_{tone} , with the pipeline illustrated in Fig. 1(b). The module operates in three sequential steps: (1) **Lip Expert Training**: A Lip Expert [14] is trained using synchronization loss calculated by a pre-trained SyncNet [14][7], with the purpose of generating Lip-wav images to initially establish audio-lip alignment. (2) **Expression Feature Extraction**: These Lip-wav images are fed into the 3D Prior Extraction sub-module [15], which extracts the expression feature f_{exp} , laying the foundation for sustained audio-vision synchronization in subsequent processing. (3) **Person-Specific Feature Fusion**: StyleNet-based audio encoder [7] is introduced to extract the person-specific complementary feature f_{tone} from the input audio. f_{tone} is then fused with f_{exp} to reconstruct 3D facial prior information $f_{gen-exp}$, ensuring the generated features retain individual identity while maintaining synchronization. The training of this part is supervised by reconstruction loss as defined by Eq. 4, with f_{gt-exp} as ground-truth.

$$L_{\text{recon}} = \|f_{gen-exp} - f_{gt-exp}\|^2 \quad (4)$$

2.2. Emotion Distillation

The Emotion Distillation module has been developed for the purpose of high-precision audio emotion extraction and strong control of emotional expressions. As shown in Fig. 1(c), this module consists of two parts: extraction and encoding.

(1) **Extraction Component**: To capture sufficient emotion information without feature dilution, we preprocess raw audio into spectrogram, MFCC, and audio-wav features [16], drawing on SER tasks [17]. We extract 2D spectrogram features via AlexNet and time-series MFCC features via LSTM, using these two as attention keys to re-weight audio-wav features into emotion-aware $f_{emo-attn}$, which supports emotion classification and expression feature prediction for downstream tasks [8, 3]. The component undergoes two training stages: pre-training on the IEMOCAP database [18] supervised by cross entropy loss of emotion labels and fine-tuning on person-specific datasets. Fine-tuning loss combines emotion label cross-entropy and L2 prediction loss between

predicted f_{emo} and ground-truth expression features f_{gt-emo} , as defined in Eq.5.

$$L_{\text{stage2}} = - \sum_{i=1}^C y_i \log(\hat{y}_i) + \|f_{emo} - f_{gt-emo}\|^2 \quad (5)$$

Where C is the number of emotion categories, y_i is the one-hot ground-truth label, and \hat{y}_i is the predicted probability. During the post-training phase, the encoder parameters are frozen to preserve extraction capability.

(2) **Encoding Component:** To handle high-dimensional emotional features incompatible with direct planar gridding [9], we adopt multi-resolution code-books [10] for discretization and replace concatenation with Hadamard product, which is validated in [19] to preserve high-dimensional information without dimension explosion. The final encoded feature $f_{emotion}$ is defined in Eq. 6.

$$f_{emotion} = \bigcup_{(s)} \prod \text{Interp}(R^s(i, j)) \odot f_{emo-attn}^s \quad (6)$$

where R is plane, $(i, j) \in \{(X, Y), (X, Z), (Y, Z)\}$, $s \in \{1, 2, 4\}$ denotes multi-resolution scales for code-book discretization, with basic resolution as 64. These scales enable precise micro-expression control for downstream Gaussian primitive deformation.

2.3. Uncertainty-based deformation

The Uncertainty-based Deformation module, composed of feature fusion and decoding components as shown in Fig. 2, addresses the flawed "one-size-fits-all" multi-view fusion issue by accounting for modality quality differences, aiming to enhance rendering quality and emotional expression precision.

(1) **Feature Fusion with Uncertainty Estimation:** For each feature view, we deploy an uncertainty block consisting of N uncertainty networks. Each network takes Gaussian primitives and the corresponding view's feature as input (except $f_{emotion}$ input alone), outputting (μ, σ) to represent the predicted distribution of the view's state vector as shown in Eq. 7.

$$p(\hat{y}_q | x_q, \theta) = \mathcal{N}(\hat{y}; \mathbf{F}_{\theta_1}^{\mu}(x), \mathbf{F}_{\theta_2}^{\sigma}(x)) \quad (7)$$

where $\mathbf{F}_{\theta_1}^{\mu}(\cdot)$ and $\mathbf{F}_{\theta_2}^{\sigma}(\cdot)$ are network branches outputting mean μ and variance σ , with trainable parameters θ_1 and θ_2 .

Following [12], uncertainty includes AU (from input noise) and EU (from model parameters) as defined in Eq. 8.

$$V[\hat{y}_q | x_q] = \underbrace{V_{q^*(\theta)}[E(\hat{y}_q | x_q, \theta)]}_{\Delta_E[\hat{y}_q]} + \underbrace{E_{q^*(\theta)}[V(\hat{y}_q | x_q, \theta)]}_{\Delta_A[\hat{y}_q]} \quad (8)$$

where $E(\hat{y}_q | x_q, \theta)$ and $V(\hat{y}_q | x_q, \theta)$ denote the mean and variance of predicted state vector \hat{y}_q under posterior predictive distribution $p(\hat{y} | x_q, \theta)$, with the left representing EU and right representing AU.

AU is directly estimated by the uncertainty network, while EU is approximated via Monte Carlo sampling: we use $T = 10$ uncertainty networks per block, calculating EU as the variance of their μ outputs. The total uncertainty for each view is formulated in Eq. 9, with the block's final output (mean $\hat{\mu}$ and variance $\hat{\sigma}$) defined in Eq. 10 and Eq. 11.

$$\begin{aligned} \hat{V}[\hat{y}_q | x_q] &= \frac{1}{T} \sum_{t=1}^T \underbrace{\mathbf{F}_{\theta_1}^{\mu}(x_q) \mathbf{F}_{\theta_1}^{\mu}(x_q)^{\top} - \bar{\mathbf{F}}^{\mu}(x_q) \bar{\mathbf{F}}^{\mu}(x_q)^{\top}}_{\hat{\Delta}_E(\hat{y}_q)} \\ &\quad + \underbrace{\sum_{t=1}^T \mathbf{F}_{\theta_2}^{\sigma}(x_q)}_{\hat{\Delta}_A(\hat{y}_q)} \end{aligned} \quad (9)$$

where $\bar{\mathbf{F}}^{\mu}(x_q) = \frac{1}{T} \sum_{t=1}^T \mathbf{F}_{\theta_1}^{\mu}(x_q)$ is the mean of output from the T networks.

$$\hat{\mu}_{y|x} = \frac{1}{T} \sum_{t=1}^T \mu_t(x; \theta_1^t) \xrightarrow{T \rightarrow \infty} \mathbb{E}_{q_{\phi}^*(y|x)}[y] \quad (10)$$

$$\hat{\sigma}_{y|x} = \frac{1}{T} \sum_{t=1}^T \left(\sigma_t(x; \theta_2^t) + \mu_t(x; \theta_1^t) \mu_t(x; \theta_1^t)^{\top} \right) - \hat{\mu}_{y|x} \hat{\mu}_{y|x}^{\top} \quad (11)$$

where $\hat{\mu}$ and $\hat{\sigma}$ are the final output of the current view.

Multi-view features are fused via Gaussian Fusion as defined in Eq. 12, where weights are dynamically adjusted by uncertainty (lower weight for higher uncertainty).

$$\mu = \Sigma \sum_{i=1}^N \hat{\sigma}_i^{-1} \hat{\mu}_i, \quad \Sigma = \left(\sum_{i=1}^N \hat{\sigma}_i^{-1} \right)^{-1} \quad (12)$$

where N is the number of input views, μ_i and σ_i are the mean and uncertainty of the i -th view's mean and uncertainty. The final output of feature fusion is predicted state vector μ , which represents audio condition of each Gaussian primitive in emotion space, with real distribution as $q_{\phi}^*(y | x)$.

(2) **Gaussian Deformation Decoding:** As shown in Fig. 2, the fused state vector is fed into a multi-head Gaussian deformation decoder, replacing conventional simple MLPs, to separately generate modification parameters $(\Delta\mu, \Delta r, \Delta s)$ for Gaussian primitives (position, rotation, scaling). This design aligns with dynamic Gaussian modeling [9], enabling fine-grained control over each primitive to improve rendering fidelity.

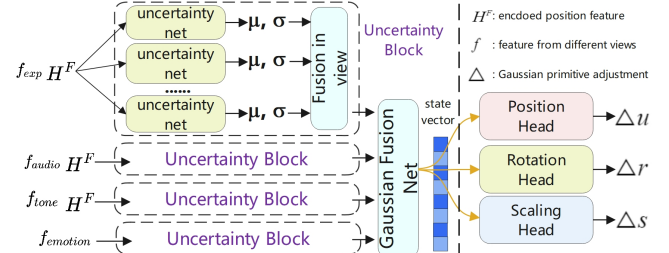


Fig. 2: Uncertainty-Based Deformation. (Left) Uncertainty-aware multi-view feature fusion module; (Right) Multi-head Gaussian deformation decoder.

2.4. UA-3DTalk Training strategy

The training process of our UA-3DTalk framework is divided into two sequential stages, ensuring the independent optimization of core modules and the effective integration of the full rendering pipeline.

Stage 1: This stage focuses on training the Prior Extraction module and pre-training the Emotion Distillation module. Detailed implementation steps for this stage are specified in their respective sections (Sections 2.1 and 2.2).

Stage 2: This stage targets the end-to-end optimization of the rendering pipeline, consisting of two key steps: First, the Uncertainty-based Deformation module is trained separately for the face and mouth branches, supervised by the loss between the ground-truth masked image \mathcal{I}_{mask} and rendered output \mathcal{I}_{render} as defined in Eq.13. Second, fine-tuning is performed to fuse the face and mouth branches, with supervision from the loss between the ground-truth image $\hat{\mathcal{I}}$ and fused output \mathcal{I}_{fuse} as shown in Eq.14.

$$\mathcal{L}_D = \mathcal{L}_1(\mathcal{I}_{render}, \mathcal{I}_{mask}) + \lambda \mathcal{L}_{SSIM}(\mathcal{I}_{render}, \mathcal{I}_{mask}) \quad (13)$$

$$\mathcal{L}_F = \mathcal{L}_1(\mathcal{I}_{fuse}, \hat{\mathcal{I}}) + \lambda \mathcal{L}_{SSIM}(\mathcal{I}_{fuse}, \hat{\mathcal{I}}) + \gamma \mathcal{L}_{LPIPS}(\mathcal{I}_{fuse}, \hat{\mathcal{I}}) \quad (14)$$

where λ and γ are both hyperparameters.

Methods	Regular / Emotion					
	LMD(\downarrow)	PSNR(\uparrow)	LPIPS(\downarrow)	SSIM(\uparrow)	Sync-C(\uparrow)	E-FID(\downarrow)
StableAvatar '25	4.117 / 7.150	18.403 / 19.290	0.258 / 0.228	0.480 / 0.619	4.421 / 3.972	0.546 / 0.430
TalkingGaussian '24	3.018 / 5.934	26.943 / 25.533	0.045 / <u>0.096</u>	<u>0.906</u> / 0.892	5.011 / 4.886	0.089 / 0.356
EDTalk '24	3.827 / 6.548	25.627 / 18.061	0.073 / 0.297	0.888 / 0.864	6.173 / 7.550	0.483 / 0.668
DEGSTalk '25	1.960 / 3.923	<u>27.104 / 28.051</u>	<u>0.042</u> / 0.162	0.891 / <u>0.924</u>	5.663 / 5.007	<u>0.076</u> / 0.154
Our	<u>2.492 / 5.407</u>	28.923 / 28.408	0.032 / 0.067	0.928 / 0.938	<u>5.750 / 5.152</u>	0.072 / 0.145
GT	-	-	-	-	7.832 / 8.163	-

Table 1: Quantitative results on both datasets. The best methods are in **bold**, and second best are with underline.

3. TRAINING AND EVALUATION

3.1. Experimental settings

Datasets. To evaluate the effectiveness of our work, experiments are conducted on two types of datasets: both regular talking face dataset [20] (including Obama and May subsets) and emotional dataset [21](using M003 and M030 subsets). For regular dataset, the input video clips are in 25 FPS, with resolution of 256×256 . For emotional dataset, the input video clips are in 30 FPS, with resolution of 512×512 .

Preprocessing. We follow the preprocessing pipeline in [7], [17] and initialization settings in [5]. To mitigate background clutter interference and camera motion, which is prominent in the MEAD dataset [21], we adopt the face window cropping method from [22].

Implementation Details. Our method is implemented on PyTorch. The structure-related hyperparameters are introduced in each subsection. In training process, we first train both the face and inside mouth branches for 50,000 iterations in parallel and then jointly fine-tune them for 10,000 iterations. We use the Adam [23] and AdamW [24] optimizers across all modules, with γ and λ in the final loss functions set to 0.2 and 0.5.

Evaluation Metrics. Model performance is evaluated by several established metrics, covering key task requirements: landmark distance (LMD) [25] for facial geometric accuracy, lip synchronization confidence score (Sync-C) [26], LPIPS [27] for high-frequency detail fidelity, SSIM [28] for facial structural consistency, and E-FID [29] for image-level emotion feature alignment.

3.2. Comparative Experiments

We compare our UA-3DTalk with four SOTA methods, including TalkingGaussian [5], DEGSTalk [30], StableAvatar [31] and EDTalk [22]. Quantitative results in Table 1 demonstrate that our method outperforms them on most metrics across both regular and emotional datasets, with 5.2% higher E-FID than EDTalk, 3.1% higher SyncC than DEGSTalk, and 0.015 lower LPIPS than competitors, achieving superior image quality. Notably, DEGSTalk with best LMD uses several ground-truth 3DMM parameters and EDTalk with competitive SyncC relies on reference videos, while our UA-3DTalk excels in pure audio-driven scenarios without such dependencies.

To further validate our UA-3DTalk’s qualitative performance, we present key frame comparisons on both datasets in Fig. 3. We highlight the mouth and eye regions (with consistent positions across rows for focused evaluation). It can be observed that our method outperforms others in three core aspects: more accurate lip synchronization, more natural eye motion control, and more precise emotion-related expression prediction. The consistency and precision of these dynamic facial regions further confirm the robustness and effectiveness of our proposed framework.

3.3. Ablation Study

We conduct an ablation study to quantify the contribution of each core module in UA-3DTalk. The tested configurations include:

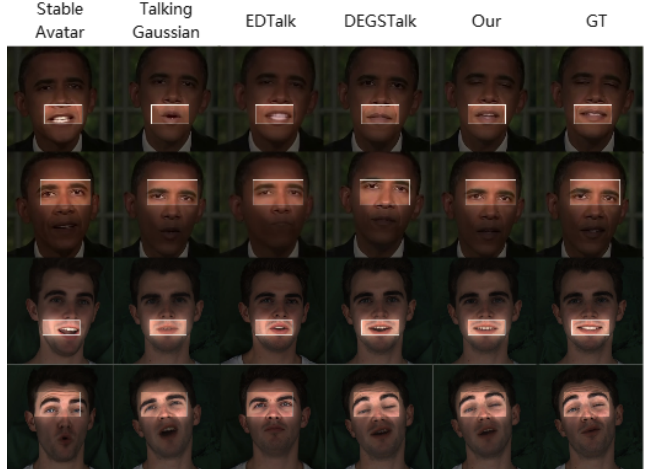


Fig. 3: Visual results of the comparative experiments.

Baseline (without any proposed modules), Prior Extraction (P), Emotion Distillation (E), and Uncertainty-based Deformation (U). Results are presented in Table 2. Notably, U cannot be implemented on the Baseline alone, this is because the Baseline only uses single-view features, while U relies on multi-view features for uncertainty estimation. Thus, we test U based on the configuration integrated with P to enable comparison with the "w/ P" setting.

	LMD \downarrow	PSNR \uparrow	LPIPS \downarrow	SSIM \uparrow	Sync-C \uparrow	E-FID \downarrow
Baseline	5.934	25.53	0.096	0.892	4.886	0.356
w/ P	<u>5.878</u>	<u>28.03</u>	<u>0.069</u>	<u>0.931</u>	<u>4.973</u>	<u>0.203</u>
w/ E	5.872	25.52	0.095	0.894	4.897	0.312
w/ P, U	5.691	28.30	0.068	0.935	5.010	0.178
w/ P, E, U	5.407	28.40	0.067	0.938	5.152	0.145

Table 2: RESULTS OF ABLATION STUDY ON MEAD

As shown in Table 2, P significantly boosts performance by generating audio-synchronized action units and expressions, validating its effectiveness. U stably enhances rendering quality without additional information, confirming the validity of our uncertainty-based fusion strategy. Though module E contributes less than module P, it clearly enhances emotion-related micro-expressions and final frames, its effectiveness is fully demonstrated by emotion expression metrics, whether used independently or with module P.

4. CONCLUSION

This paper proposes UA-3DTalk to solve two key challenges in 3D emotional talking face synthesis: difficult audio emotion extraction with weak expression control, and flawed "one-size-fits-all" multi-view fusion. It is the first to integrate uncertainty modeling in this field, with its Prior Extraction and Emotion Distillation modules enhancing audio-vision emotion alignment. Experiments show UA-3DTalk achieves state-of-the-art performance, outperforming SOTA methods by 5.2% in E-FID, 3.1% in SyncC, and 0.015 in LPIPS.

5. ACKNOWLEDGEMENT

This work is supported by the Noncommunicable Chronic Diseases-National Science and Technology Major Project (2024ZD0525800).

6. REFERENCES

- [1] Rebecca Mobbs, Dimitrios Makris, and Vasileios Argyriou, “Emotion recognition and generation: A comprehensive review of face, speech, and text modalities,” 2025.
- [2] Shuai Tan, Bin Ji, and Ye Pan, “Flowvqtalker: High-quality emotional talking face generation through normalizing flow and quantization,” in *Proceedings of the IEEE/CVF Conference on Computer Vision and Pattern Recognition (CVPR)*, June 2024, pp. 26317–26327.
- [3] Haotian Wang, Yuzhe Weng, Yueyan Li, Zilu Guo, Jun Du, Shutong Niu, Jiefeng Ma, Shan He, Xiaoyan Wu, Qiming Hu, Bing Yin, Cong Liu, and Qingfeng Liu, “Emotivetalk: Expressive talking head generation through audio information decoupling and emotional video diffusion,” in *Proceedings of the IEEE/CVF Conference on Computer Vision and Pattern Recognition (CVPR)*, June 2025, pp. 26212–26221.
- [4] Zhilei Liu, Xiaoxing Liu, Sen Chen, Jiaxing Liu, Longbiao Wang, and Chongke Bi, “Multimodal fusion for talking face generation utilizing speech-related facial action units,” *ACM Trans. Multimedia Comput. Commun. Appl.*, vol. 20, no. 9, Sept. 2024.
- [5] Jiahe Li, Jiawei Zhang, Xiao Bai, Jin Zheng, Xin Ning, Jun Zhou, and Lin Gu, “Talkinggaussian: Structure-persistent 3d talking head synthesis via gaussian splatting,” *arXiv preprint arXiv:2404.15264*, 2024.
- [6] Xinya Ji, Hang Zhou, Kaisiyuan Wang, Qianyi Wu, Wayne Wu, Feng Xu, and Xun Cao, “Eamm: One-shot emotional talking face via audio-based emotion-aware motion model,” in *ACM SIGGRAPH 2022 Conference Proceedings*, New York, NY, USA, 2022, SIGGRAPH ’22, Association for Computing Machinery.
- [7] Xiaoxing Liu, Zhilei Liu, and Chongke Bi, “Nerf-3dtalker: Neural radiance field with 3d prior aided audio disentanglement for talking head synthesis,” in *ICASSP 2025 - 2025 IEEE International Conference on Acoustics, Speech and Signal Processing (ICASSP)*, 2025, pp. 1–5.
- [8] Duomin Wang, Yu Deng, Zixin Yin, Heung-Yeung Shum, and Baoyuan Wang, “Progressive disentangled representation learning for fine-grained controllable talking head synthesis,” in *Proceedings of the IEEE/CVF Conference on Computer Vision and Pattern Recognition (CVPR)*, June 2023, pp. 17979–17989.
- [9] Guanjun Wu, Taoran Yi, Jiemin Fang, Lingxi Xie, Xiaopeng Zhang, Wei Wei, Wenyu Liu, Qi Tian, and Xinggang Wang, “4d gaussian splatting for real-time dynamic scene rendering,” in *Proceedings of the IEEE/CVF Conference on Computer Vision and Pattern Recognition (CVPR)*, June 2024, pp. 20310–20320.
- [10] Shuai Shen, Wanhua Li, Yunpeng Zhang, Yap-Peng Tan, and Jiwen Lu, “Audio-plane: Audio factorization plane gaussian splatting for real-time talking head synthesis,” 2025.
- [11] Yifan Xie, Fei Ma, Yi Bin, Ying He, and Fei Yu, “Audio-driven talking face video generation with joint uncertainty learning,” 2025.
- [12] Riccardo Barbano, Simon Arridge, Bangti Jin, and Ryutaro Tanno, “Chapter 26 - uncertainty quantification in medical image synthesis,” in *Biomedical Image Synthesis and Simulation*, The MICCAI Society book Series, pp. 601–641. Academic Press, 2022.
- [13] Ryutaro Tanno, Aurobrata Ghosh, Francesco Grussu, Enrico Kaden, Antonio Criminisi, and Daniel C. Alexander, ”, in *Medical Image Computing and Computer-Assisted Intervention – MICCAI 2016*, Cham, 2016, pp. 265–273, Springer International Publishing.
- [14] K R Prajwal, Rudrabha Mukhopadhyay, Vinay P. Namboodiri, and C.V. Jawahar, “A lip sync expert is all you need for speech to lip generation in the wild,” in *Proceedings of the 28th ACM International Conference on Multimedia*, New York, NY, USA, 2020, MM ’20, p. 484–492, Association for Computing Machinery.
- [15] Wenxuan Zhang, Xiaodong Cun, Xuan Wang, Yong Zhang, Xi Shen, Yu Guo, Ying Shan, and Fei Wang, “Sadtalker: Learning realistic 3d motion coefficients for stylized audio-driven single image talking face animation,” in *Proceedings of the IEEE/CVF Conference on Computer Vision and Pattern Recognition (CVPR)*, June 2023, pp. 8652–8661.
- [16] Alexei Baevski, Henry Zhou, Abdelrahman Mohamed, and Michael Auli, “wav2vec 2.0: a framework for self-supervised learning of speech representations,” in *Proceedings of the 34th International Conference on Neural Information Processing Systems*, Red Hook, NY, USA, 2020, NIPS ’20, Curran Associates Inc.
- [17] Heqing Zou, Yuke Si, Chen Chen, Deepu Rajan, and Eng Siong Chng, “Speech emotion recognition with co-attention based multi-level acoustic information,” in *ICASSP 2022 - 2022 IEEE International Conference on Acoustics, Speech and Signal Processing (ICASSP)*, 2022, pp. 7367–7371.
- [18] Carlos Busso, Murtaza Bulut, Chi-Chun Lee, Abe Kazemzadeh, Emily Mower, Samuel Kim, Jeannette N. Chang, Sungbok Lee, and Shrikanth S. Narayanan, “Iemocap: Interactive emotional dyadic motion capture database,” *Language Resources and Evaluation*, vol. 42, no. 4, pp. 335–359, 2008.
- [19] Sara Fridovich-Keil, Giacomo Meanti, Frederik Rahbæk Warburg, Benjamin Recht, and Angjoo Kanazawa, “K-planes: Explicit radiance fields in space, time, and appearance,” in *Proceedings of the IEEE/CVF Conference on Computer Vision and Pattern Recognition (CVPR)*, June 2023, pp. 12479–12488.
- [20] Yudong Guo, Keyu Chen, Sen Liang, Yong-Jin Liu, Hujun Bao, and Juyong Zhang, “Ad-nerf: Audio driven neural radiance fields for talking head synthesis,” in *Proceedings of the IEEE/CVF International Conference on Computer Vision (ICCV)*, October 2021, pp. 5784–5794.
- [21] Kaisiyuan Wang, Qianyi Wu, Linsen Song, Zhuoqian Yang, Wayne Wu, Chen Qian, Ran He, Yu Qiao, and Chen Change Loy, “Mead: A large-scale audio-visual dataset for emotional talking-face generation,” in *ECCV*, August 2020.
- [22] Shuai Tan, Bin Ji, Mengxiao Bi, and Ye Pan, “Edtalk: Efficient disentanglement for emotional talking head synthesis,” in *Computer Vision – ECCV 2024*, Cham, 2025, pp. 398–416, Springer Nature Switzerland.
- [23] Diederik P. Kingma and Jimmy Ba, “Adam: A method for stochastic optimization,” 2017.
- [24] Ilya Loshchilov and Frank Hutter, “Decoupled weight decay regularization,” 2019.
- [25] Lele Chen, Zhiheng Li, Ross K Maddox, Zhiyao Duan, and Chenliang Xu, “Lip movements generation at a glance,” in *Proceedings of the European Conference on Computer Vision (ECCV)*, September 2018.
- [26] Joon Son Chung and Andrew Zisserman, “Out of time: Automated lip sync in the wild,” in *Computer Vision – ACCV 2016 Workshops*, Cham, 2017, pp. 251–263, Springer International Publishing.
- [27] Richard Zhang, Phillip Isola, Alexei A. Efros, Eli Shechtman, and Oliver Wang, “The unreasonable effectiveness of deep features as a perceptual metric,” in *Proceedings of the IEEE Conference on Computer Vision and Pattern Recognition (CVPR)*, June 2018.
- [28] Zhou Wang, A.C. Bovik, H.R. Sheikh, and E.P. Simoncelli, “Image quality assessment: from error visibility to structural similarity,” *IEEE Transactions on Image Processing*, vol. 13, no. 4, pp. 600–612, 2004.
- [29] Linrui Tian, Qi Wang, Bang Zhang, and Liefeng Bo, “Emo: Emote portrait alive generating expressive portrait videos with audio2video diffusion model under weak conditions,” in *Computer Vision – ECCV 2024*, Cham, 2025, pp. 244–260, Springer Nature Switzerland.
- [30] Kaijun Deng, Dezhong Zheng, Jindong Xie, Jinbao Wang, Weicheng Xie, Linlin Shen, and Siyang Song, “Degstalk: Decomposed per-embedding gaussian fields for hair-preserving talking face synthesis,” in *ICASSP 2025 - 2025 IEEE International Conference on Acoustics, Speech and Signal Processing (ICASSP)*, 2025, pp. 1–5.
- [31] Shuyuan Tu, Yueming Pan, Yimeng Huang, Xintong Han, Zhen Xing, Qi Dai, Chong Luo, Zuxuan Wu, and Yu-Gang Jiang, “Stableavatar: Infinite-length audio-driven avatar video generation,” 2025.